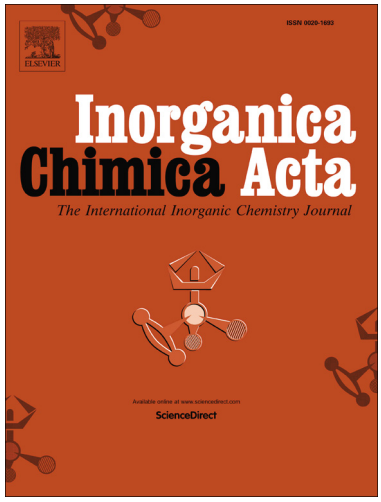

Research paper

Highly Selective and Efficient Solvent-free Transformation of Bio-derived Levulinic acid to γ-Valerolactone by Ru(II) Arene Catalyst Precursors

Novisi K. Oklu, Banothile C.E. Makhubela

PII: S0020-1693(18)30831-4
DOI: https://doi.org/10.1016/j.ica.2018.06.050
Reference: ICA 18342

To appear in: *Inorganica Chimica Acta*

Received Date: 29 May 2018
Revised Date: 27 June 2018
Accepted Date: 28 June 2018

Please cite this article as: N.K. Oklu, B.C.E. Makhubela, Highly Selective and Efficient Solvent-free Transformation of Bio-derived Levulinic acid to γ-Valerolactone by Ru(II) Arene Catalyst Precursors, *Inorganica Chimica Acta* (2018), doi: https://doi.org/10.1016/j.ica.2018.06.050

Highly Selective and Efficient Solvent-free Transformation of Bio-derived Levulinic acid to γ-Valerolactone by Ru(II) Arene Catalyst Precursors

Novisi K. Oklu[a] and Banothile C. E. Makhubela[a*]

[a]*Department of Chemistry, University of Johannesburg, Auckland Park Kingsway Campus*

P.O. Box 524, South Africa, Johannesburg

[*]E-mail: bmakhubela@uj.ac.za

ABSTRACT

The selective and efficient solvent-free hydrogenation of bio-based levulinic acid (LA) to γ-valerolactone (GVL) was achieved with new pyridylimine ruthenium(II) complexes as catalyst precursors. The hydrogenation reactions were performed in the presence of formic acid as hydrogen source using a catalyst loading as low as 0.1 mol% with potassium hydroxide or triethylamine (Et_3N). 4-Hydroxyvaleric acid (HVA) was produced only when KOH was used, whereas reactions involving Et_3N were selective to GVL. At 150 °C, >96 % LA conversions were achieved with 100 % GVL selectivity. Recyclability of catalyst precursors was demonstrated by running three consecutive reactions where 100 % conversion and selectivity was maintained. In-situ NMR studies show that hydrogen gas is formed by the decomposition of formic acid to carbon dioxide and hydrogen. Ru-hydride species have been detected, by ^1H NMR, and are believed to be the catalytically active species, and a mechanism of the reaction has been proposed.

KEYWORDS

Solvent-free reactions; formic acid; hydrogen generation; levulinic acid; gamma-valerolactone; arene ruthenium(II) complexes

ABBREVIATIONS

γ-Valerolactone: GVL

Levulinic acid: LA

4-Hydroxyvaleric acid: 4-HVA

Triethylamine: Et_3N

Formic acid: FA

Hydroxymethylfurfural: HMF

1. INTRODUCTION

Liquid fuels as well as most chemicals and polymers that are currently used are derived from petroleum. However, due to high demand for petroleum products, crude oil reserves are heading towards rapid depletion [1]. The problems of environmental pollution and climate impacts often linked to the burning of fossil resources (crude oil, natural gas and coal), are also of concern [2]. Over the past 50 years, atmospheric carbon dioxide concentrations have risen by about 30 % and this has been accompanied by a rise in other Green House Gases, including CH_4 and NO_2. This has caused about 0.6 °C increase in the average temperature of the earth's surface [3]. As such, renewable alternative sources of energy and chemical resources need to be developed to meet the growing demands [2]. One of such potential alternative feedstock is biomass [4]. Non-edible, lignocellulosic or 'wood-based', biomass has gained attention recently. It is a complex carbohydrate polymer, which is mainly made up of cellulose (41 %), hemicellulose (28 %) and lignin (27 %) [4,5]. This lignocellulosic biomass can be transformed into many chemicals including ethanol, *n*-butanol, sorbitol, hydroxymethylfurfural, dimethylfuran and γ-valerolactone (GVL) [6,7].

GVL has gained much attention over the past few decades due to its attractive physical and chemical characteristics as well as its unique fuel characteristics [8]. It has low toxic levels, an acceptable and definitive smell which makes detection of leaks and spills easy, high flash point (96 °C), high boiling (207 °C) point, low melting point (-31 °C), and above all, it is obtained from a renewable source. It is also used as an additive in the food industry [9]. This has made GVL to stand out as one of the most promising renewable platform molecules that can be transformed into various chemicals, such are valeric acid, 1,4-pentanediol, 2-methyl tetrahydrofuran and 2-butene. In turn, GVL serves as an intermediate in the production of a broad range of biofuels as well as commodity and fine chemicals [7,10].

GVL can be produced from cellulose and sugars by first hydrolyzing waste cellulose to glucose followed by glucose ↔ to fructose isomerization. Fructose can then be converted to hydroxymethylfurfural (HMF) via dehydration. This is followed by rehydration of the HMF to levulinic acid (LA). LA is further hydrogenated to GVL using metal catalysts with an external hydrogen source, or formic acid (FA) as the source of hydrogen (**Scheme 1**). Using FA as the source of hydrogen is more economical in this case because hydrolysis of glucose

produces FA in equimolar amounts to LA. In the presence of a catalyst, FA decomposes into CO_2 and H_2 and hence can be used as an internal source of hydrogen (**Scheme 1**) [11].

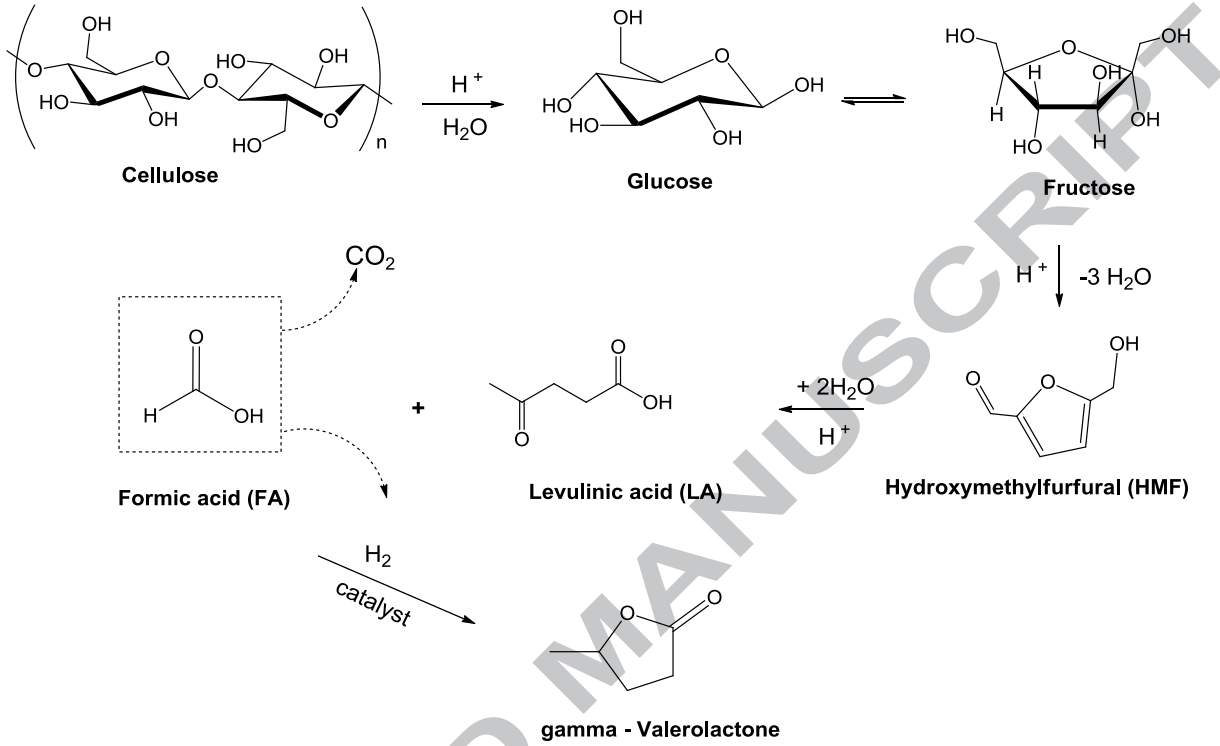

Scheme 1: Production of GVL from LA using FA or molecular hydrogen [5-9].

Recently, much effort has been put into the development of heterogeneous catalytic systems, such as Ru, Ni, Rh, Ir, Pt and Pd on carbon and oxides, for the conversion of LA to GVL [12–14]. However, it has been shown that for the hydrogenation of bio-sourced molecules, including the conversion of LA to GVL, ruthenium metal particles supported on various carbons and oxides, such as 5 % Ru/C, 5 % Ru/SiO_2 and 5 % Ru/Al_2O_3, were the most efficient catalysts to achieve a fast and selective conversion [15,16]. With regards to ruthenium metal particles supported on oxides, Luo and co-workers studied the influence that supports of different acidities (Nb_2O_5, TiO_2, H-ZSM5 and H-β) have on the activity and selectivity of the hydrogenation of LA using ruthenium, and found that supports with higher amounts of Lewis acid sites gave higher conversions [17].

Even though heterogeneous catalysts have the advantages of easy separation and recycling of the catalyst, the homogeneous catalysts have very efficient activities and are also highly selective under relatively mild conditions [9,12]. In the transformation of LA to GVL, water-soluble homogeneous catalysts have been increasingly attractive. Especially because GVL

does not form an azeotropic mixture with water, hence the catalyst can be recovered for reuse, through distillation [18].

Furthermore, studies have shown that homogeneous catalysts have higher activities in the decomposition of FA to produce hydrogen gas [19]. Some of the metal complexes used in this regard include those with Pd [19], Ir [20,21], Fe [22], Rh [23] and Ru [24] metal centers. Deng *et. al.*, reported the use of FA as a source of hydrogen for the conversion of LA to GVL in the presence of a mixture of $RuCl_3$ (0.2 mol%) and PPh_3 (0.6 mol%) catalyst. They proposed that the formic acid is decomposed to hydrogen gas which is then used for the hydrogenation of the LA [25] as opposed to going through the transfer hydrogenation process with Shvo catalysts proposed by Horvath *et al*. [26] Recently, we reported the transformation of LA to GVL with FA as a source of hydrogen in the presence of pyrazolylphophinite and pyrazolylphosphite-ruthenium (II) complexes bearing *p*-cymene auxiliary ligand. In situ ^{1}HNMR studies showed that the reaction proceeds by the production of molecular hydrogen and carbon dioxide gases from FA [27]. Hence, it can be deduced that homogeneous ruthenium catalysts have the added advantage of both facilitating the production of hydrogen gas from FA as well as converting LA to GVL.

While much research has been carried out on the development of water-soluble phosphines, hydrophilic nitrogen ligands have received relatively little attention [28]. It has however been reported that nitrogen donor ligands, such as Schiff bases in particular, are able to stabilize many different metals in different oxidation states and as such control the activity of metals in various transformations [29,30]. A recent study reported the use of half-sandwich ruthenium(II) complexes with Schiff base ligands in the transfer hydrogenation of ketones to alcohols. Sodium formate was employed as the hydrogen source for the reaction which resulted in yields greater than 95 % [31a]. In view of this, ruthenium hydrogenation catalyst systems, especially those derived from nitrogen donor ligands, may be of interest in the conversion of LA to GVL. In this work, we report the synthesis of new Schiff base N^N donor ligands and their use in the solvent-free hydrogenation of LA to GVL, using FA as a source of hydrogen. The highly selective synthesis of GVL was achieved by using pyridylimine ruthenium(II) complexes as catalyst precursors. The use of FA (which is produced as a by-product in the manufacture of LA) [31b] as the source of hydrogen and the absence of solvent, make this an appealing and green way for GVL production.

2. MATERIALS AND METHODS

2.1 General information

4-aminobenzoic acid (99 %), 2-pyridinecarboxylic acid (99 %), 2-quinolinecarboxaldehyde (97 %), 2-aminopyridine (98 %), 4-formylbenzoic acid (97 %), 4-(aminomethyl)-benzoic acid (97 %), dichloro(*p*-cymene)ruthenium(II)dimer, 1,5-cyclooctadiene (COD) (98 %), $RuCl_3 \cdot xH_2O$, levulinic acid (97 %) and formic acid (95 %) were all purchased from Sigma-Aldrich and were used as supplied. All solvents used were of analytical grade and were dried using MBRAUN SPS-800 solvent drying system. **L1** [33] and **L2** [34] were prepared according to literature methods. The metal precursor $[RuCl_2(COD)]_n$ was synthesized following reported literature method [32]. ^{1}H NMR (400 MHz) and $^{13}C\{^1H\}$ NMR (100 MHz) spectra were recorded on a Bruker-400 MHz spectrometer and values were reported relative to tetramethylsilane (δ 0.0) as internal standard. FT-IR spectra were recorded using a Perkin Elmer FT-IR Spectrum BX-ATR. Elemental analyses were performed on a Thermo Scientific FLASH 2000 CHNS-O analyzer. HR-MS (ESI) spectra were recorded on a Waters Synapt G2 spectrometer. Melting points were determined using a Gallenkamp digital melting point apparatus. All hydrogenation reactions were performed in PPV-CTRO1-CE high pressure reactor vessels fitted into a high pressure autoclave reactor with-in built stirring, heating and cooling systems.

2.2 Synthesis of (E)-4-((quinolin-2-ylmethylene)amino)benzoic acid (L3)

2-Quinolinecarboxaldehyde (0.510 g, 3.24 mmol) was dissolved in hot dry ethanol (15 ml), followed by the addition of 4 drops of formic acid. 4-Aminobenzoic acid (0.231 g, 1.68 mmol) was then added. The solution formed was refluxed for 2 h after which the solvent was removed by using a rotary evaporator to afford a brown solid. Dry dichloromethane (15 ml) was then added to the solid to form a suspension. The suspension was filtered and the residue washed with dry dichloromethane (10 ml) to afford a pale brown solid which was dried overnight under vacuum. Yield: 0.328g (70.50 %); M.p: 210 - 213 °C; FT-IR (ν_{max}/cm^{-1}): 2892 b (OH), 1708 s (C=O), 1597 s (HC=N), 1566 w (C=N); ^{1}H NMR (400 MHz, DMSO-d_6, 25 °C, δ, ppm): 10.10 (s, 1H, -OH), 8.70 (s, 1H, imine-CH), 8.50 (d, $^3J_{HH}$ = 8.80 Hz, 1H, quin-CH), 8.30 (d, $^3J_{HH}$ = 8.80 Hz, 1H, quin-CH), 8.10 (d, $^3J_{HH}$ = 6.40 Hz, 1H, quin-CH), 8.08 (d, $^3J_{HH}$ = 8.00 Hz, 1H, quin-CH), 8.03 (d, $^3J_{HH}$ = 8.40 Hz, 2H, aromatic-CH), 7.80 (t, $^3J_{HH}$ = 6.80 Hz, 1H, quin-CH), 7.70 (t, $^3J_{HH}$ = 7.20 Hz, 1H, quin-CH), 7.40 (d, $^3J_{HH}$ = 8.40 Hz, 2H, aromatic-CH); $^{13}C\{^1H\}$ NMR (100 MHz, DMSO-d_6, 25 °C, δ, ppm): 166.92 (-

COOH), 162.55 (imine-C=N), 154.19 (aromatic-C-N), 154.01, 147.38 (quin-C=N), 137.18 (quin-CH), 130.67 (aromatic-CH), 130.37 (quin-CH), 129.30 (quin-CH), 128.92, 128.58 (aromatic-C(COOH)), 128.20 (quin-CH), 128.14 (quin-CH), 121.23 (aromatic-CH), 118.28 (quin-CH); CHN-calculated: (73.90 % C, 4.38 % H, 10.14 % N), CHN-obtained: (73.47 % C, 4.24 % H, 9.81 % N); HR-MS (ESI^+) $C_{17}H_{13}N_2O_2$ calculated, *m/z* = 277.0977 $[M+H]^+$, found, *m/z* = 277.0967 $[M+H]^+$; Solubility: DMSO, hot methanol and ethanol.

2.3 Synthesis of [Ru(p-cymene)Cl(L1)]Cl (1)

A mixture of **L1** (122.16 mg, 0.540 mmol) and [Ru(*p*-cymene)Cl_2]$_2$ (165.36 mg, 0.270 mmol) in dry methanol (20 mL) was transferred into a schlenk tube. The tube was deaerated with nitrogen gas and the solution stirred at room temperature for 20 h. After 20 h, the solvent was removed by rotary evaporation to afford an orange solid product which was dried overnight *in vacuo*. Yield: (270 mg, 93.9 %); M.p: decomposes without melting (onset at 180 °C); FT-IR (ν_{max}/cm^{-1}): 3380 b (OH), 1702 s (C=O), 1600 s (HC=N); ^{1}H NMR (400 MHz, MeOD-d_4, 25 °C, δ, ppm): 9.53 (d, $^3J_{HH}$ = 5.60 Hz, 1H, pyr-CH), 8.84 (s, 1H, imine-CH), 8.31 – 8.25 (m, 4H, pyr-CH, pyr-CH, aromatic-CH), 7.89 (d, $^3J_{HH}$ = 8.40 Hz, 2H, aromatic-CH), 7.86 (t, $^3J_{HH}$ = 5.60 Hz, 1H, pyr-CH), 6.00 (d, $^3J_{HH}$ = 6.00 Hz, 1H, *p*-cym-CH), 5.69 (d, $^3J_{HH}$ = 6.00 Hz, 1H, *p*-cym-CH), 5.64 (d, $^3J_{HH}$ = 6.00 Hz, 1H, *p*-cym-CH), 5.50 (d, $^3J_{HH}$ = 6.40 Hz, 1H, *p*-cym-CH), 2.60 (m, $^3J_{HH}$ = 7.20 Hz, 1H, *p*-cym-CH(CH_3)$_2$), 2.25 (s, 3H, *p*-cym-CH_3), 1.09 (d, $^3J_{HH}$ = 6.80 Hz, 6H, *p*-cym-CH_3); $^{13}C\{^1H\}$ NMR (100 MHz, DMSO-d_6, 25 °C, δ, ppm): 206.41 (-COOH), 168.94 (imine-C=N), 166.48 (pyridyl-C=N), 156.15 (pyr-CH), 154.72, 154.38 (aromatic-C(COOH)), 139.94 (pyr-CH), 130.64 (aromatic-CH), 130.50 (pyr-CH), 129.11 (pyr-CH), 122.76 (aromatic-CH), 105.24 (*p*-cym-C(CH_3)), 103.71, 86.67 (*p*-cym-CH), 86.00 (*p*-cym-CH), 84.87 (*p*-cym-CH, *p*-cym-CH), 30.45 ((*p*-cym-C(CH_3)$_2$)), 21.67 (*p*-cym-CH_3, *p*-cym-CH_3), 18.26 (*p*-cym-CH_3); CHN-calculated: (51.88 % C, 4.56 % H, 5.26 % N), CHN-obtained: (52.26 % C, 4.53 % H, 4.96 % N); HR-MS (ESI^+) $[C_{23}H_{24}ClN_2O_2Ru]^+$ calculated, *m/z* = 497.0570 $[M]^+$, found, *m/z* = 497.0570 $[M]^+$; Solubility: water, methanol, ethanol.

2.4 Synthesis of [Ru(p-cymene)Cl(L2)]Cl (2)

The synthesis was performed as for **1** by using **L2** (129.60 mg, 0.540 mmol) and [Ru(*p*-cymene)Cl_2]$_2$ (165.36 mg, 0.270 mmol). Yield: (0.237 g, 80.34 %); M.p: decomposes without melting (onset at 175 °C); FT-IR (ν_{max}/cm^{-1}): 3385 b (OH), 1705 s (C=O), 1611 s (HC=N),

1473 w (C=N); ^{1}H NMR (400 MHz, DMSO-d_6, 25 °C, δ, ppm): 13.133 (s, 1H, -COOH), 9.55 (d, $^{3}J_{HH}$ = 5.20 Hz, 1H, pyr-CH), 8.51 (s, 1H, imine-CH), 8.24 – 8.19 (m, 2H, pyr-CH, pyr-CH), 8.02 (d, $^{3}J_{HH}$ = 8.0 Hz, 2H, aromatic-CH), 7.79 (t, $^{3}J_{HH}$ = 6.00 Hz, 1H, pyr-CH), 7.61 (d, $^{3}J_{HH}$ = 8.00 Hz, 2H, aromatic-CH), 6.25 (d, $^{3}J_{HH}$ = 6.00 Hz, 1H, *p*-cym-CH), 6.06 (d, $^{3}J_{HH}$ = 5.60 Hz, 1H, *p*-cym-CH), 5.90 (d,$^{3}J_{HH}$ = 6.8 Hz, 1H, *p*-cym-CH), 5.88 (d,$^{3}J_{HH}$ = 6.4 Hz, 1H, *p*-cym-CH), 5.80 (d, $^{3}J_{HH}$ = 16.00 Hz, 1H, -CH_2), 5.56 (d, $^{3}J_{HH}$ = 16 Hz, 1H, -CH_2), 2.49 (m, 1H, *p*-cym-CH(CH_3)$_2$), 2.08 (s, 3H, *p*-cym-CH_3), 0.98 (d, $^{3}J_{HH}$ = 6.80 Hz, 3H, *p*-cym-CH_3), 0.90 (d, $^{3}J_{HH}$ = 6.80 Hz, 3H, *p*-cym-CH_3); ^{13}C{^{1}H} NMR (100 MHz, DMSO-d_6, 25 °C, δ, ppm): 206.41 (-COOH), 168.39 (imine-C=N), 167.46 (-C(CH_2)), 156.50 (pyr-CH), 154.91 (pyridyl-C=N), 139.49 (pyr-CH), 131.48 (aromatic-C(COOH)), 130.62 (aromatic-CH), 130.31 (aromatic-CH), 129.87 (pyr-CH), 128.84 (pyr-CH), 105.08 (*p*-cym-C(CH_3)), 103.76, 87.97 (*p*-cym-CH), 84.96 (*p*-cym-CH), 84.83 (*p*-cym-CH), 84.73 (*p*-cym-CH), 68.71 (-CH_2), 30.89 (*p*-cym-C(CH_3)$_2$), 22.51 (*p*-cym-CH_3), 21.94 (*p*-cym-CH_3), 18.80 (*p*-cym-CH_3); CHN-calculated: (52.75 % C, 4.80 % H, 5.13 % N), CHN-obtained: (53.06 % C, 4.65 % H, 5.28 % N); HR-MS (ESI^{+}) $[C_{24}H_{26}ClN_2O_2Ru]^{+}$ calculated, *m/z* = 511.0726 $[M]^{+}$, found, *m/z* = 511.0737 $[M]^{+}$; Solubility: water, methanol, ethanol.

2.5 Synthesis of [Ru(p-cymene)Cl(L3)]Cl (3)

Complex **3** was prepared following a procedure similar to that reported for **1** by using **L3** (99.48 mg, 0.360 mmol) and [Ru(*p*-cymene)Cl_2]$_2$ (110.24 mg, 0.180 mmol). Yield: (193 mg, 91.90 %); M.p: decomposes without melting (onset at 187 °C); FT-IR (ν_{max}/cm^{-1}): 3387 b (OH), 1706 s (C=O), 1593 s (HC=N), 1513 w (C=N); ^{1}H NMR (400 MHz, MeOD-d_4, 25 °C, δ, ppm): 9.09 (s, 1H, imine-CH), 8.85 (d, $^{3}J_{HH}$ = 8.40 Hz, 1H, quin-CH), 8.82 (d, $^{3}J_{HH}$ = 8.80 Hz, 1H, quin-CH), 8.33 (d, $^{3}J_{HH}$ = 8.40 Hz, 1H, quin-CH), 8.32 (d, $^{3}J_{HH}$ = 8.40 Hz, 2H, aromatic-CH), 8.28 (d, $^{3}J_{HH}$ = 8.40 Hz, 1H, quin-CH), 8.20 (t, $^{3}J_{HH}$ = 7.60 Hz, 1H, quin-CH), 8.06 (d, $^{3}J_{HH}$ = 8.80 Hz, 2H, aromatic-CH), 8.01 (t, $^{3}J_{HH}$ = 7.20 Hz, 1H, quin-CH), 6.03 (d, $^{3}J_{HH}$ = 6.40 Hz, 1H, *p*-cym-CH), 5.89 (d, $^{3}J_{HH}$ = 6.00 Hz, 1H, *p*-cym-CH), 5.77 (d, $^{3}J_{HH}$ = 6.40 Hz, 1H, *p*-cym-CH), 5.32 (d, $^{3}J_{HH}$ = 6.00 Hz, 1H, *p*-cym-CH), 2.38 (m, $^{3}J_{HH}$ = 7.20 Hz, 1H, *p*-cym-CH(CH_3)$_2$), 2.29 (s, 3H, *p*-cym-CH_3), 0.99 (d, $^{3}J_{HH}$ = 6.80 Hz, 3H, *p*-cym-CH_3), 0.84 (d, $^{3}J_{HH}$ = 6.80 Hz, 3H, *p*-cym-CH_3); ^{13}C{^{1}H} NMR (100 MHz, DMSO-d_6, 25 °C, δ, ppm): 206.92 (-COOH), 170.34 (imine-C=N), 166.98 (pyridyl-C=N), 156.09, 155.55 (aromatic-C(COOH)), 148.92, 141.37 (quin-CH), 133.93 (quin-CH), 132.51, 131.27 (aromatic-CH), 130.99 (quin-CH), 129.80 (quin-CH, quin-CH), 125.39 (quin-CH), 123.23

(aromatic-CH), 106.01 (*p*-cym-C(CH_3)), 105.54, 87.01 (*p*-cym-CH), 86.82 *p*-cym-CH), 85.98 (*p*-cym-CH), 85.09 (*p*-cym-CH), 30.95 (*p*-cym-C(CH_3)$_2$), 22.51 (*p*-cym-CH_3), 21.43 (*p*-cym-CH_3), 18.78 (*p*-cym-CH_3); CHN-calculated: (55.67 % C, 4.50 % H, 4.81 % N), CHN-obtained: (56.00 % C, 4.56 % H, 4.75 % N); HR-MS (ESI$^+$) $[C_{27}H_{26}ClN_2O_2Ru]^+$ calculated, *m/z* = 547.0726 $[M]^+$, found, *m/z* = 547.0725 $[M]^+$; Solubility: water, methanol, ethanol.

2.6 Synthesis of [Ru(COD)Cl$_2$(L1)] (4)

A mixture of **L1** (81.4 mg, 0.36 mmol) and the ruthenium polymer (100 mg, 0.36 mmol) in dry ethanol (10 mL) was transferred into a schlenk tube. The tube was deaerated with nitrogen gas and the mixture refluxed with stirring for 2 h. The solution was then reduced to about a third of the original volume and kept overnight at 4 °C to allow precipitation. The resulting dark solution was carefully decanted off to afford a brown precipitate. Cold ethanol (10 mL) was added to the precipitate and then filtered off. Further washing of the brown precipitate was done with cold ethanol (10 mL) followed by diethyl ether (10 mL). The brown precipitate was dissolved in 5 mL chloroform followed by the addition of excess *n*-hexane (20 mL) to induce precipitation of the product. Finally, the precipitated product was obtained by filtration and washed with *n*-hexane (10 mL) to afford a brown solid product which was dried overnight under vacuum. Yield: (158 mg, 87.00 %); M.p: decomposes without melting (onset at 260 °C); FT-IR (ν_{max}/cm^{-1}): 3035 b (OH), 1721 s (C=O), 1598 s (HC=N), 1497 w (C=N); ^{1}H NMR (400 MHz, DMSO-d$_6$, 25 °C, δ, ppm): 13.10 (s, 1H, -COOH), 8.90 (s, 1H, imine-CH), 8.30 (d, $^3J_{HH}$ = 5.20 Hz, 1H, pyr-CH), 8.28 (d, $^3J_{HH}$ = 6.80 Hz, 1H, pyr-CH), 8.23 (t, $^3J_{HH}$ = 7.20 Hz, 1H, pyr-CH), 8.00 (d, $^3J_{HH}$ = 8.00 Hz, 2H, aromatic-CH), 7.70 (t, $^3J_{HH}$ = 6.00 Hz, 1H, pyr-CH), 7.30 (d, $^3J_{HH}$ = 8.40 Hz, 2H, aromatic-CH), 4.50 (s, 2H, cod-CH), 3.80 (s, 2H, cod-CH), 2.00 (m, 3H, cod-CH_2), 1.90 (m, 3H, cod-CH_2); ^{13}C{^{1}H} NMR (100 MHz, DMSO-d$_6$, 25 °C, δ, ppm): 170.79 (imine-C=N), 166.71 (pyridyl-C=N), 156.17, 152.50 (aromatic-C(COOH)), 150.91 (pyr-CH), 139.13 (pyr-CH), 130.30 (aromatic-CH), 129.78 (pyr-CH), 128.67 (pyr-CH), 121.03 (aromatic-CH), 90.20 (COD-CH), 89.73 (COD-CH), 29.33 (COD-CH_2), 28.93 (COD-CH_2); CHN-calculated: (49.81 % C, 4.38 % H, 5.53 % N), CHN-obtained: (49.33 % C, 4.39 % H, 5.16 % N); HR-MS (ESI$^+$) $C_{21}H_{21}N_2O_2Ru$ calculated, *m/z* = 435.0725, found, *m/z* = 435.0639 $[M\text{-}H\text{-}2Cl]^+$; Solubility: DMSO.

2.7 General procedure for hydrogenation reactions

Levulinic acid (20 mmol), formic acid (20 mmol), catalyst (0.02 mmol / 0.1 mol %), and base (Et_3N/KOH) (20 mmol) were added to an autoclave reactor. The mixture was heated to the desired temperature after purging four times with nitrogen gas. The mixture was then left to stir for the required length of time. At the end of the reaction, the reactor vessel was cooled and the gas generated released. A sample of the mixture was then analysed by ^{1}H NMR. All hydrogenation reactions were carried out in triplicates.

3. RESULTS AND DISCUSSION

3.1 Synthesis and characterisation of ligands L1 to L3

The ligands were prepared as shown in (**Scheme 2**) and characterised using ^{1}H NMR, ^{13}C{^{1}H} NMR, elemental analysis (CHN) and mass spectroscopy. The ^{1}H NMR spectrum of the compounds show characteristic signals for the imine proton between 8.20 and 8.60 ppm. This was further corroborated by absorption bands between 1590 and 1690 cm^{-1} in the infrared spectra of **L1** to **L3**. The IR spectra of the ligands also show absorption bands between 1560 and 1590 cm^{-1} which correspond to the C=N stretching frequency of the pyridyl moiety.

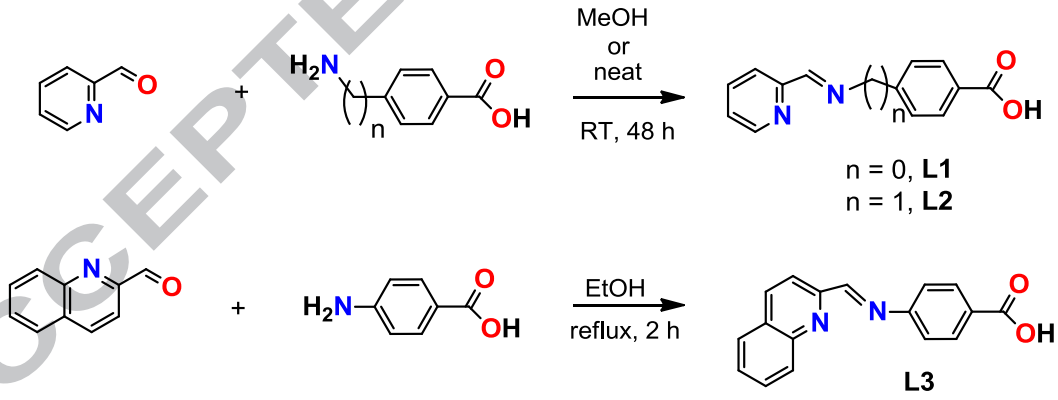

Scheme 2: Outline of the syntheses of ligands **L1** to **L3**.

3.2 Synthesis and characterisation of complexes 1 to 3

Complexes **1** – **3** were synthesized by the reaction of the appropriate ligands (**L1** to **L3**) with [$RuCl_2$(*p*-cymene)]$_2$ at room temperature for 20 h. Complex **4** was synthesized by refluxing **L1** with [$RuCl_2$(1,5-cyclooctadiene)]$_n$ in methanol for 24 h (**Scheme 3**). All complexes were

characterised using ^{1}H and $^{13}C\{^{1}H\}$ NMR spectroscopy, elemental analysis (CHN), infrared spectroscopy and mass spectrometry. The ^{1}H NMR spectrum of the complexes show significant shifts of the signal for the imine protons as well as those adjacent to the pyridyl nitrogen. The shifts in these proton signals serve as a confirmation that both nitrogen atoms have coordinated to the ruthenium centre by displacing a chloride which serves as a counter ion to the complex. The signals of the four aromatic protons of the *p*-cymene moiety in complexes **1**–**3** were expected to appear as two doublets if the *p*-cymene sits on a perpendicular plane to the metal. However, the signals appeared as four separate peaks each appearing as a doublet. This could be due to the fact that the *p*-cymene moiety loses its symmetry upon coordination of the N^N donor ligand to the metal. A similar trend has been reported in literature, where an imine and amine nitrogen atoms were coordinated to a ruthenium with a *p*-cymene ligand [35].

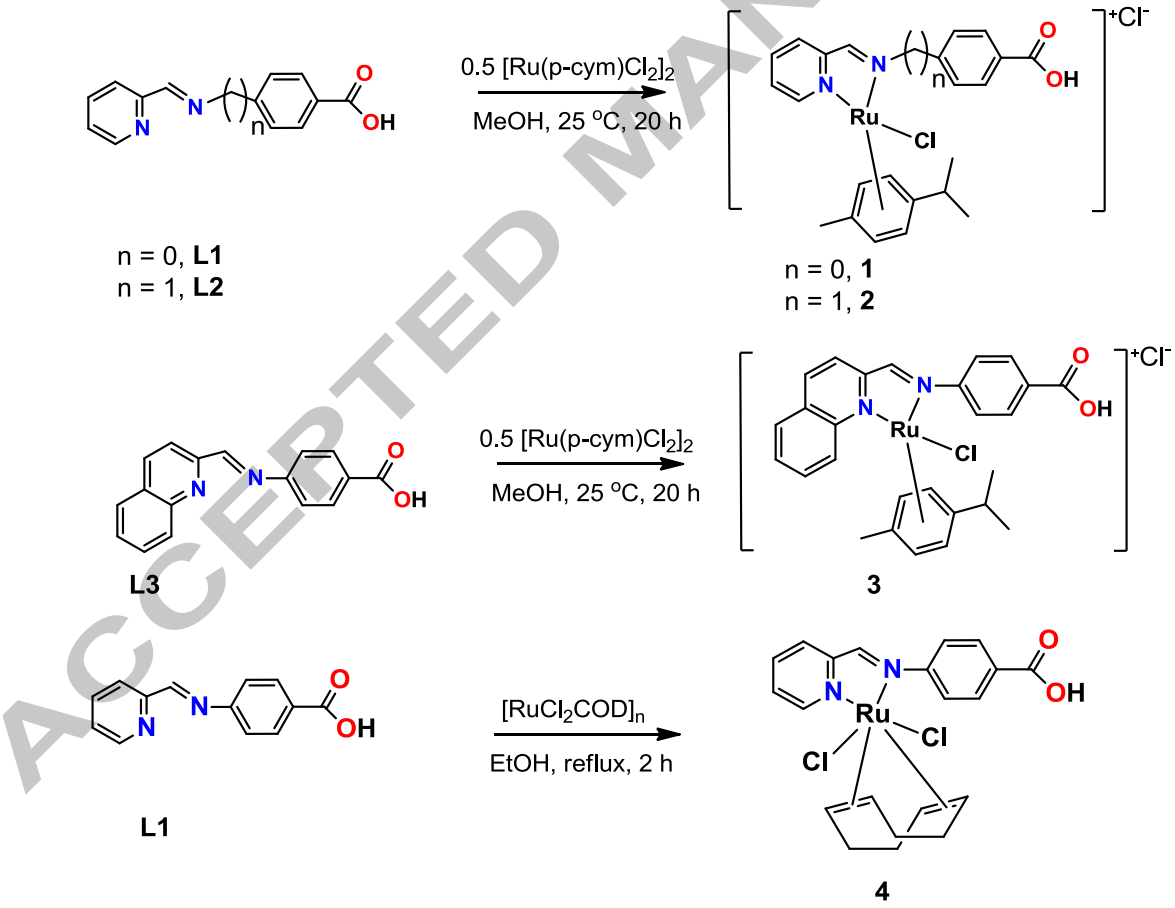

Scheme 3: Outline for the syntheses of complexes **1** to **4**.

In addition, the methylene protons adjacent to the imine nitrogen in complex **3** have split into two separate peaks appearing at 5.80 ppm and 5.56 ppm. This can also be attributed to loss of symmetry. The $[M]^{+}$ peaks, which correspond to the cationic part of the complexes, were

observed in the mass spectra of complexes **1** to **3**. In the mass spectrum of complex **4**, a peak is observed at *m/z* = 435.0639 $[C_{21}H_{21}N_2O_2Ru]^+$, which corresponds to the mass of **4** minus hydrochloric acid and a chloride ligand. This indicates that, unlike **1**-**3**, this compound fragments easily under the conditions that the mass spectra were collected.

3.3 Hydrogenation of LA with formic acid

The reactions were performed under solvent-free conditions by reacting levulinic acid (20 mmol), formic acid (20 mmol), catalyst (0.02 mmol), and KOH (20 mmol) in an autoclave reactor at 150 °C for 12 h (**Table 1**). Catalyst precursor **4** gave the highest conversion (96 %) followed by **3** (93 %), **2** (59 %) and **1** (45 %) (**Table 1**, entries 1 – 4). The intermediate, 4-HVA, was also produced in addition to GVL, with pre-catalysts **1**, **2**, **3** and **4** giving 4-HVA selectivities of 66 %, 34 %, 58 % and 47 % respectively. The reactions were repeated with a reduced amount of KOH (2 mmol) which resulted in reduced conversions (**Table 1**, entries 5 – 8). Pre-catalyst **3** recorded the highest conversion (42 %) followed by **2** (24 %) as well as **4** and **1** with conversions of 20 % and 14 % respectively. Interestingly, when the amount of KOH was reduced to 2 mmol, the only product detected was GVL. This shows that the pre-catalysts are selective to only GVL at lower amounts of KOH. However, higher conversion of LA can be achieved at higher amounts of KOH but with the production of both GVL and the 4-HVA intermediate.

Table 1: Hydrogenation of LA using formic acid and KOH**.**

Entry	**Cat.**[c]	**LA Conversion** (%)[b]	**GVL Selectivity** (%)[b]	**4-HVA Selectivity** (%)[b]
1	**1**	45	34	66
2	**2**	59	66	34
3	**3**	93	42	58
4	**4**	96	53	47
5[a]	**1**	14	100	0
6[a]	**2**	24	100	0
7[a]	**3**	42	100	0

8[a]	**4**	20	100	0

Conditions: LA (20 mmol), formic acid (20 mmol), catalyst (0.02 mmol), KOH (20 mmol), 12 h, 150 °C.[25] **[a]** 2 mmol of KOH was added. **[b]** Conversion and Selectivity determined by ^{1}H NMR spectroscopy.**[c]** Cat. = catalyst precursor; Average error estimates: ±0.44 (**1**), ±0.49 (**2**), ±0.53 (**3**), ±0.57 (**4**).

When Et_3N was used (**Table 2**, entries 1 – 4), all pre-catalysts gave conversions above 96 % with **3** and **4** giving the highest conversion (97 %). The reaction was also repeated with less amount of Et_3N (2 mmol) (**Table 2**, entries 5 – 8) but the conversions observed did not differ much from when 20 mmol of Et_3N was used. Pre-catalyst **2** only showed the lowest conversion (36 %) when small amount of Et_3N was used. Pre-catalyst **3** gave the highest conversion (98 %) followed by **4** and **1** with 93 % conversions each. This shows that the pre-catalysts only require small amounts of Et_3N in performing the transformation of levulinic acid to GVL selectively.

Table 2: Hydrogenation of LA using formic acid and Et_3N.

Entry	**Cat.**[f]	**LA Conversion** (%)[e]	**GVL Selectivity** (%)[e]	**4-HVA Selectivity** (%)[e]
1	**1**	96	100	0
2	**2**	96	100	0
3	**3**	97	100	0
4	**4**	97	100	0
5[d]	**1**	93	100	0
6[d]	**2**	36	100	0
7[d]	**3**	98	100	0
8[d]	**4**	93	100	0

Conditions: LA (20 mmol), formic acid (20 mmol), catalyst (0.02 mmol), Et_3N (20 mmol), 12 h, 150 °C.[25] **[d]** 2 mmol of Et_3N was added. **[e]** Conversion and Selectivity determined by ^{1}H NMR spectroscopy. **[f]** Cat. = catalyst precursor; Average error estimates: ±0.52 (**1**), ±0.49 (**2**), ±0.37 (**3**), ±0.47 (**4**).

The results from these preliminary screening show that, for the selected conditions, the pre-catalysts perform better with organic bases than with inorganic bases, possibly due to lack of solubility of the KOH. Wang *et.al.*, reported 99 % yield with 1 equivalent Et_3N and 2 equivalent FA in 16 h, when ruthenium catalysts bearing dipyridyl-amine ligands were used to synthesize GVL from LA and formic acid [36]. Our catalysts require only 0.1 equivalent Et_3N together with 1 equivalent FA to achieve yields from 96 – 97 % in 12 h. The reactions were also carried out without the presence of a base [37a] and the conversions of LA for each catalyst was poor, indicating that the base is necessary for the reaction. Also, when the reaction was repeated without catalyst [37a], only 10 % conversion of LA was observed. This confirms that the hydrogenation reactions are being catalyzed by the ruthenium. We chose catalytic amounts of base (0.1 equivalent Et_3N) over stoichiometric amounts (1 equivalent) as the optimal amount of base for the hydrogenation reactions and this was used for all subsequent reactions.

3.4 Conversion as a function of time

The reactions were performed using 0.1 equivalents Et_3N for 2 h, 4 h, 8 h, 12 h and 16 h. All pre-catalysts have an induction period of 2 to 4 h (**Figure 1**). The conversions with **1**, **3** and **4** gradually increased after 4 h to greater than 90 % in 16 h, with **4** being the highest (99 %). Pre-catalyst **2**, however, has a shorter induction period and recorded a conversion of 65% even after16 h.

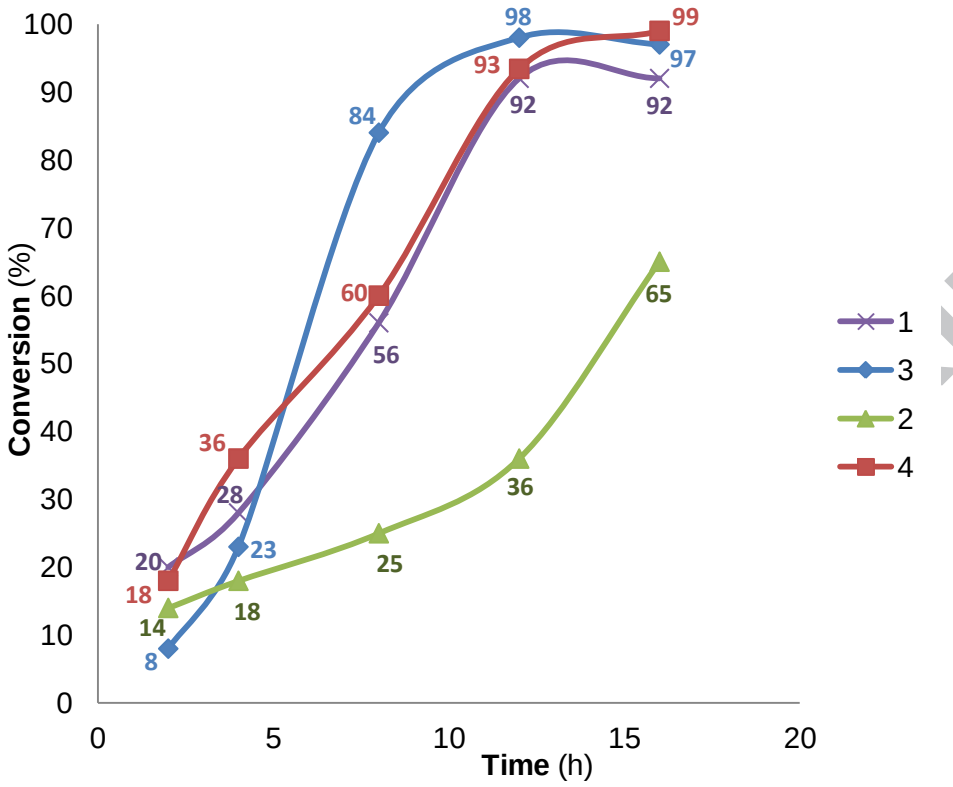

Figure 1: Time dependence studies of the hydrogenation of LA using formic acid. Conditions: LA (20 mmol), formic acid (20 mmol), catalyst (0.02 mmol), Et_3N (2 mmol) and 150 °C. ; Average error estimates: ±0.24 (**1**), ±0.49 (**2**), ±0.33 (**3**), ±0.42 (**4**).

The low activity of **2** can be explained by comparing its structural difference to **1**. The only difference between the two compounds is the added methylene group between the imine nitrogen and the aromatic group in **3**. It is possible that the degree of freedom about the methylene group may cause flexibility, therefore allowing the aromatic group to fold over and prevent easy access to the ruthenium active center. This steric bulk around the ruthenium center could hinder the coordination of the formate to the metal center, which is the first step of the reaction. It was interesting to observe 100 % selectivity to GVL regardless of how long the reaction had proceeded for all the catalyst precursors (**Figure 2**). From the above results, 16 h was taken as the optimum time for further reactions.

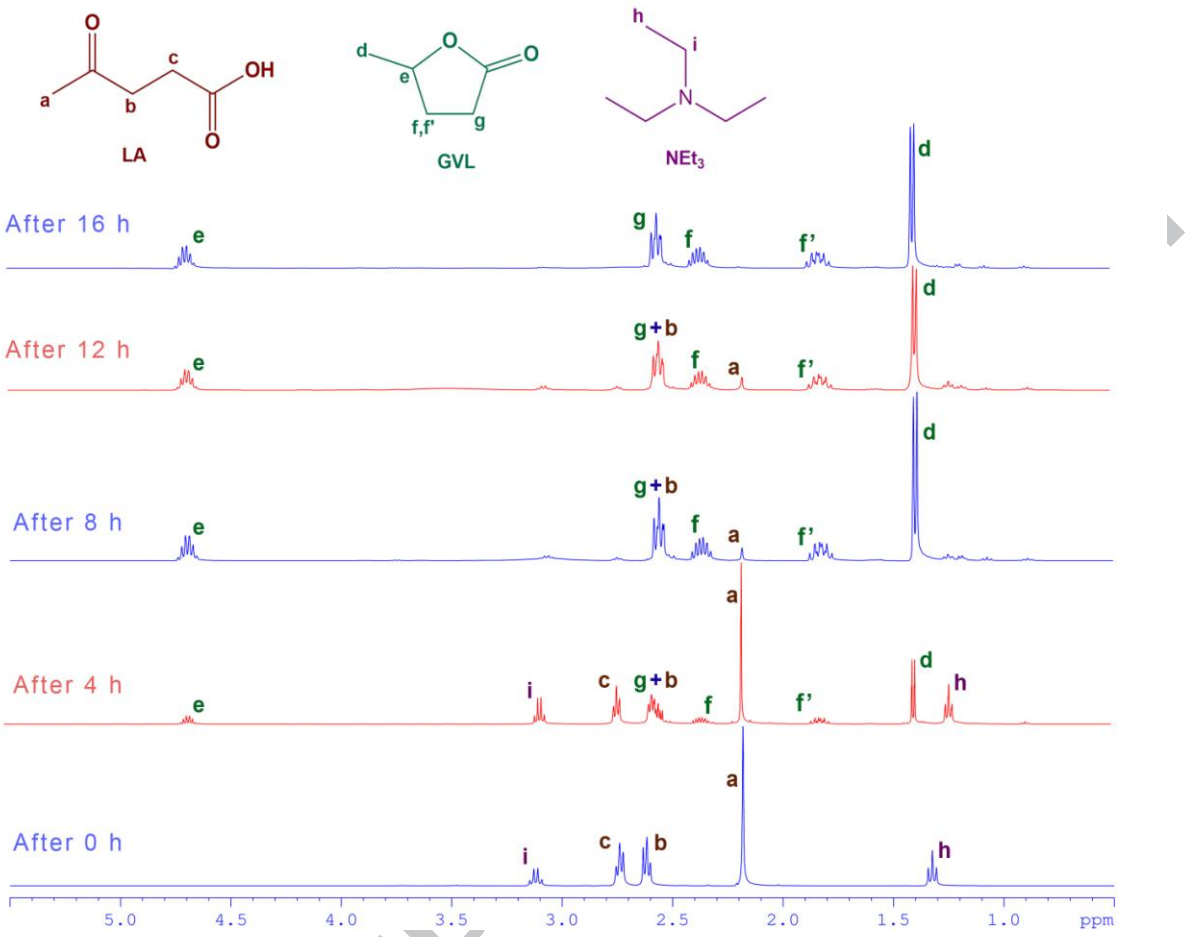

Figure 2: ^{1}H NMR spectra of hydrogenation reactions with **4**

Conditions: LA (20 mmol), formic acid (20 mmol), catalyst (0.02 mmol), Et_3N (2 mmol), 150 °C.

3.5 Effect of temperature

Varying the temperature from 125 °C to 175 °C (**Figure 3**) resulted in increased conversion for all pre-catalysts, while the selectivity was maintained at 100 % GVL. At 125 °C, all pre-catalysts gave conversions below 30 %, with the exception of **3** which gave a conversion of 88 %. At 175 °C, **3** and **4** gave complete conversions of LA to afford GVL. Thus, pre-catalyst **3** is the best performing catalyst since it maintains activity even at a lower temperature of 125 °C.

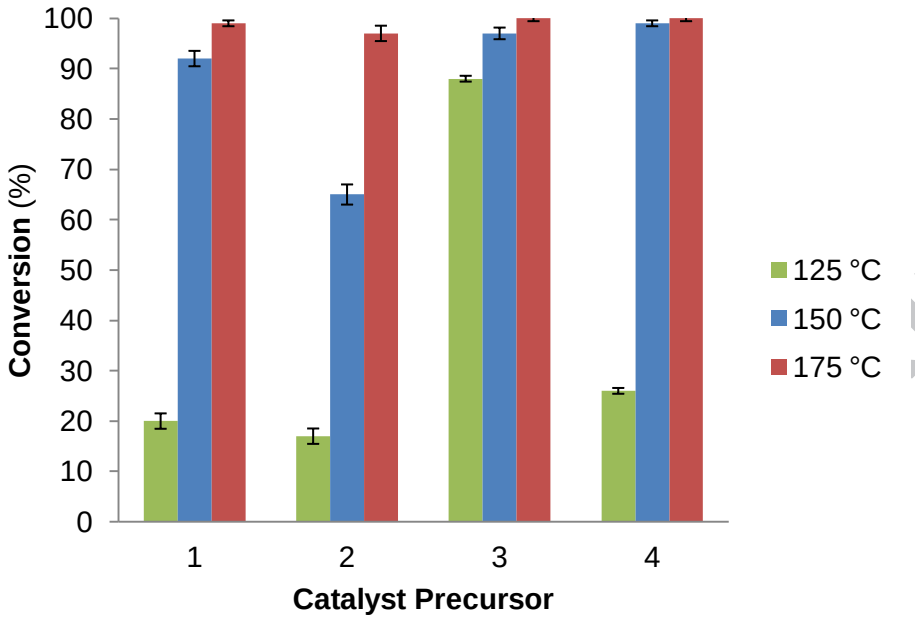

Figure 3: Effects of temperature on the hydrogenation of LA using formic acid. Conditions: LA (20 mmol), formic acid (20 mmol), catalyst (0.02 mmol), Et_3N (2 mmol), 16 h.

3.6 Mercury poisoning tests

Homogeneity test was performed for pre-catalysts **3** and **4** in the hydrogenation of LA to GVL for 16 h at 175 °C using metallic mercury, where 2 mg of metallic mercury was dropped in the reaction vessel. This was done to poison any nanoparticles that might be formed, during the reaction, and subsequently promote the conversion. Our experiments show that there is no significant change in conversion for both pre-catalysts in the presence of mercury. LA conversions with **3** and **4** dropped from 100 % to 98 % and 97 % respectively (**Figure 4**), thus confirming that the active species generated from the pre-catalysts, are of a homogeneous nature.

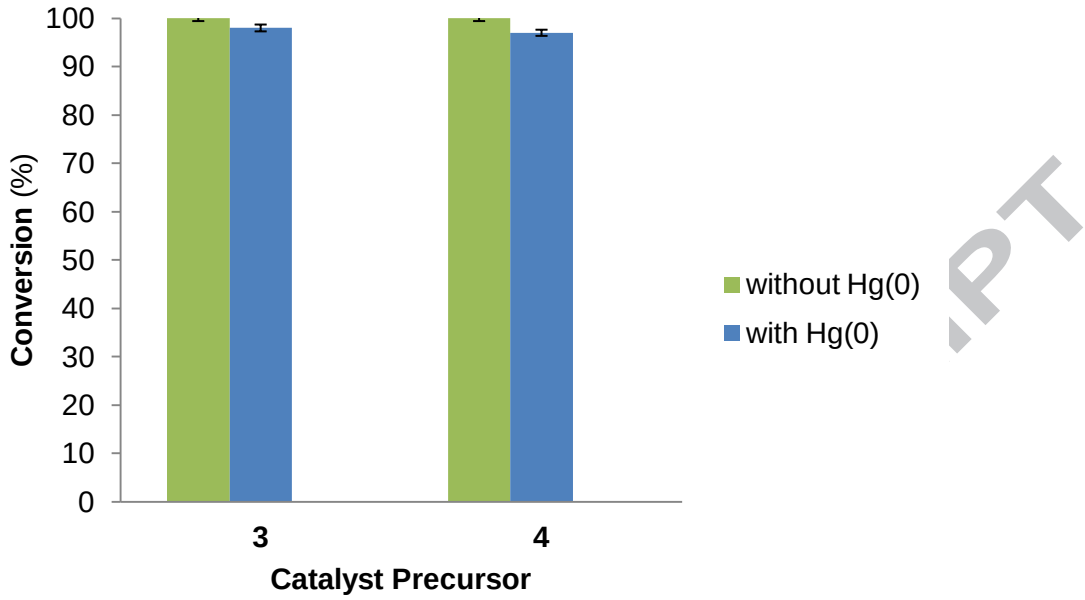

Figure 4: Mercury drop test of **3** and **4** in the hydrogenation of LA using formic. Conditions: LA (20 mmol), formic acid (20 mmol), catalyst (0.02 mmol), Et_3N (2 mmol), Hg(0) (2 mg), 16 h, 175 °C.

3.7 Recyclability of 3 and 4

Recyclability of **3** and **4** (which were the best performing catalyst precursors) was investigated at 175 °C for 16 h (**Figure 5**). At the end of the reaction, the crude mixture was dissolved in ethanol and transferred into a Schlenk tube. The resulting solution was evaporated off under vacuum at 90 °C, leaving behind the catalyst [26]. Ethanol was then used to wash the catalyst back into the autoclave reactor, followed by drying in a vacuum oven at 40 °C. After the ethanol was completely removed, the reactor was recharged with LA, FA and Et_3N. The mixture was then heated at 175 °C for 16 h. The procedure was repeated until the fifth run. For both **3** and **4**, 100 % conversion of LA and 100 % selectivity to GVL was maintained until the third run. However, for **3**, the conversion reduced to 75 % and 22 % in the fourth and fifth runs respectively, whereas that of **4** was reduced to 97 % and 61 % in the fourth and fifth runs respectively. This effectively indicates that for both pre-catalysts, deactivation occurs after the fourth run with the rate of deactivation occurring faster for **3** than **4**. It is well known that ruthenium-arene complexes bearing chloride ligands readily undergo chloride ligand substitution with aqua ligands in the presence of water. Therefore, deactivation of the pre-catalyst may be due the formation of inactive oxo-bridging

species [35,37b], which can easily be accessed from pre-formed ruthenium aqua complexes, where the water is derived from the cyclization of 4-HVA to GVL.

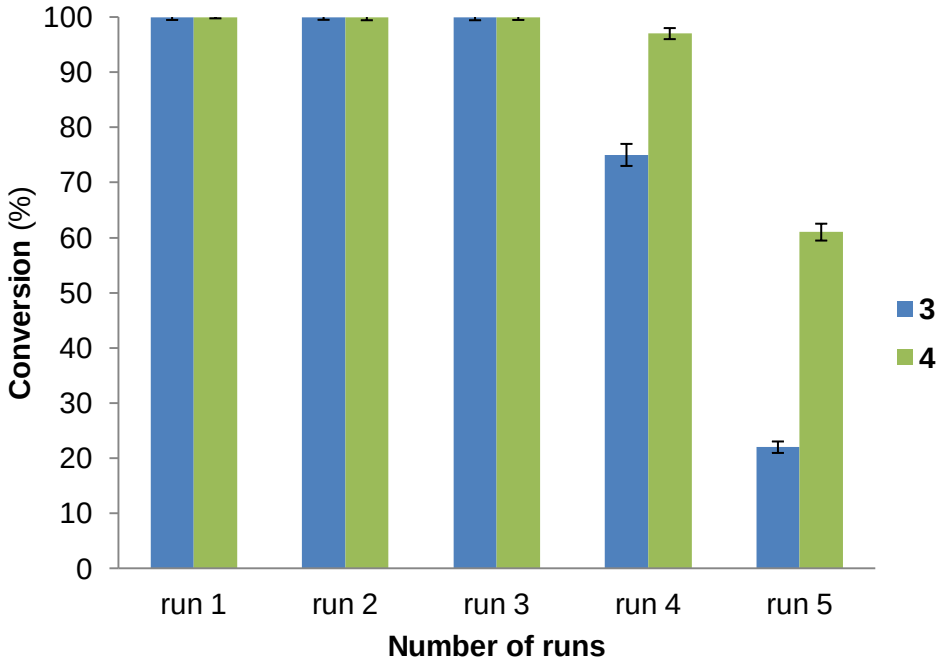

Figure 5: Recyclability test of **3** and **4** in the hydrogenation LA using formic. Conditions: LA (20 mmol), formic acid (20 mmol), catalyst (0.02 mmol), Et_3N (2 mmol), 16 h, 175 °C.

3.8 In-situ NMR studies

The catalytic reaction was monitored by performing a small scale reaction in MeOD-d_4 in a J Young NMR tube. Levulinic acid, formic acid, Et_3N and pre-catalyst **1** were loaded into the J Young NMR tube and heated in an oil bath at 125 °C. After 30 min, the ^{1}H NMR spectrum showed the formation of hydrogen gas as a result of decomposition of formic acid [37b]. The chemical shift at 8.12 ppm, which was from the formic acid, disappeared completely after 30 min, with a simultaneous appearance of a new singlet at 4.47 ppm which corresponds to hydrogen gas. Deng *et al.*, also reported the formation of hydrogen gas after 20 min, when they reacted in situ generated active catalytic species from $RuCl_3 \cdot 3H_2O$ and PPh_3 with LA and FA in the presence of Et_3N, albeit without ^{1}H NMR evidence [25]. ^{1}H NMR evidence of the decomposition of formic acid has, however, been reported with Pd [19] and Ru [27] catalysts. In addition to the formation of hydrogen gas, there was cleavage of the Ru – imine nitrogen bond [37c]. There was disappearance of the signals of the pre-catalyst **1** and the

appearance of new peaks upfield. Also, the aromatic protons of the *p*-cymene which originally appeared as four separate peaks now coalesced at around 5.55 – 5.59 ppm. This bond cleavage could be to allow formate ion to coordinate to the metal center as a first step in formic acid decomposition. Studies have shown that the catalytic decomposition of formic acid in the absence of tertiary amines is very slow [38]. Another small scale reaction was performed by loading formic acid, Et_3N and pre-catalyst **1** into a J Young NMR tube, and this was heated in an oil bath at 125 °C. Again, the ^{1}H NMR spectrum [37d] showed the complete disappearance of the chemical shift of the formic acid which initially appears as a singlet at 8.10 ppm. A new singlet at 4.45 ppm also appeared, corresponding to hydrogen gas. Additionally, the same peak patterns that indicate the cleavage of the Ru-imine nitrogen bond were observed. This goes on to support that the hydrogenation reaction proceeds by the ruthenium catalyzed decomposition of formic acid to generate hydrogen gas. Evidence of Ru-hydride species formation was observed in the negative region of the ^{1}H NMR (**Scheme 4**).

3.9 Proposed reaction mechanism

The proposed mechanism for the hydrogenation reaction is shown in **Scheme 4**. Formate ion is first formed by the deprotonation of formic acid by Et_3N. In **Pathway A**, the formate ion coordinates to the metal center of pre-catalyst **1** after the Ru–imine nitrogen bond cleavage. This is the first step in the Ru-catalyzed formic acid decomposition to form carbon dioxide and hydrogen gas. Molecular hydrogen then coordinates to the metal centre as shown in **1**(**I**) which can quickly form a Ru-hydride species **1**(**III**), with the expulsion of HCl. Ru-assisted transfer of hydrogen to the ketone end of levulinic acid, to from **1**(**VI**) is followed by the formation of intermediate **1(V)**. After 4-HVA and CO_2 are released a second molecule of formate coordinates to the coordinatively unsaturated species **1(VI)**, this then produces intermediate **1(II)** again and leads to regeneration of the active species **1**(**III**). 4-HVA undergoes lactonization to form GVL with the loss of a water molecule. In **Pathway B**, an anion metathesis between the formate ion and the chloride ion on the ruthenium center of pre-catalyst **1** occurs. Once the metathesis has taken place, triethylammonium chloride is released and intermediate **1(II)** is formed. A hydride is abstracted from the formate which is coordinated to ruthenium via its charged oxygen atom. This results in the active species **1(III)** which then undergoes the same reaction steps as in **Pathways A**.

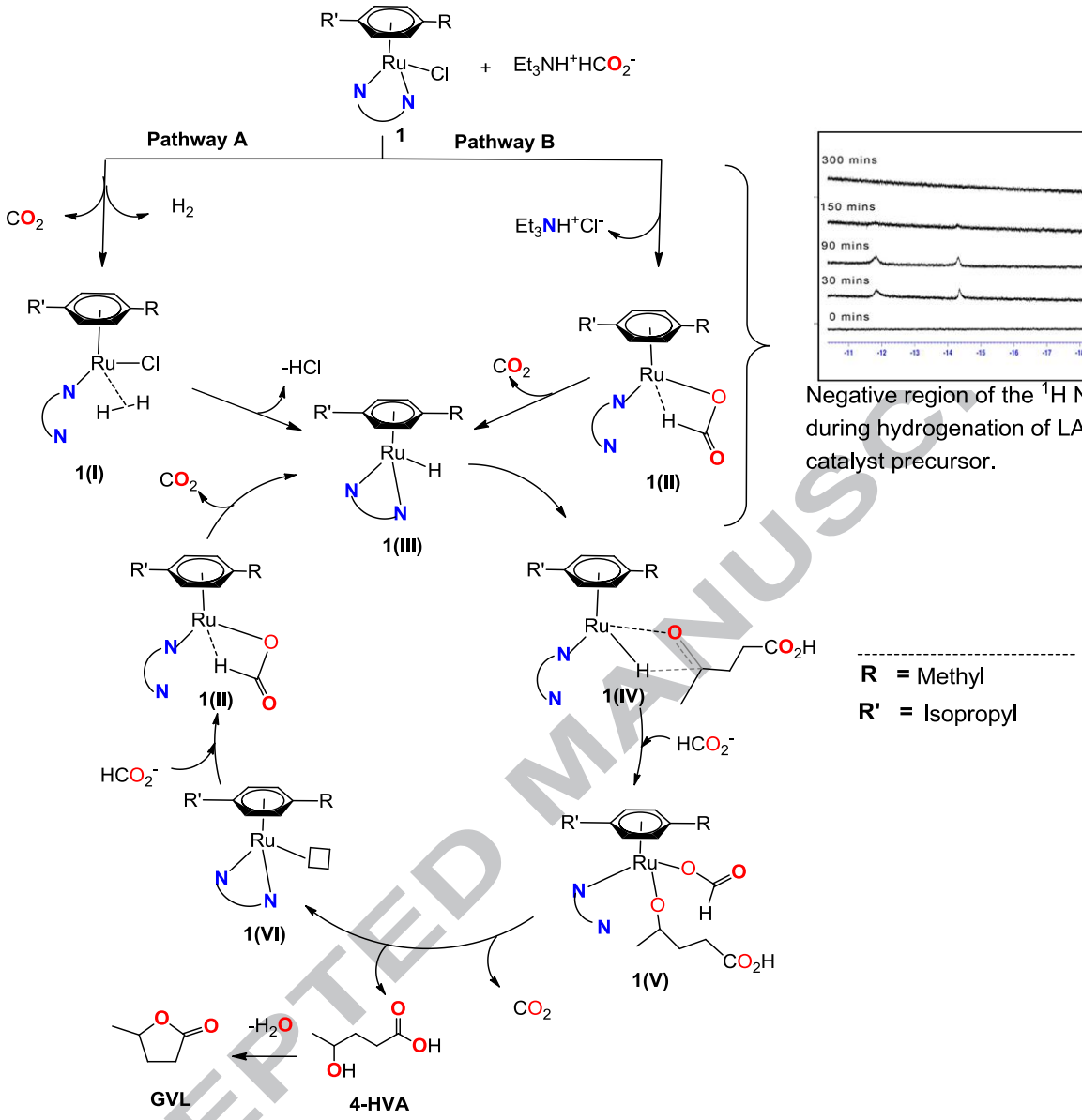

Negative region of the ^{1}H NMR spectrum during hydrogenation of LA, using **1** as the catalyst precursor.

Scheme 4: Proposed catalytic mechanism.

3.10 Aqueous media hydrogenation of LA

The process of transformation of cellulose to levulinic acid results in the formation of an aqueous mixture of formic acid and levulinic acid (**Scheme 1**) [39]. 15 wt% aqueous solution of glucose was converted to LA (42 wt%) and formic acid (17 wt%), by acid catalyzed dehydration with 0.8 M HCl at 220 °C [25]. This was done with the aim of achieving direct conversion of glucose to GVL in aqueous media. Once the LA and formic acid has formed, it would be easy to then add the hydrogenation catalyst without having to remove water. For this to be practical, the pre-catalyst would have to be effective in aqueous media. As such,

we then conducted the hydrogenation reactions in 50 wt% distilled water at 125 °C for 16 h [37e]. Conversions of levulinic acid decreased as compared to when the reactions were performed solvent-free. A further decrease in conversions was observed when the temperature was increased to 175 °C (**Figure 6**).

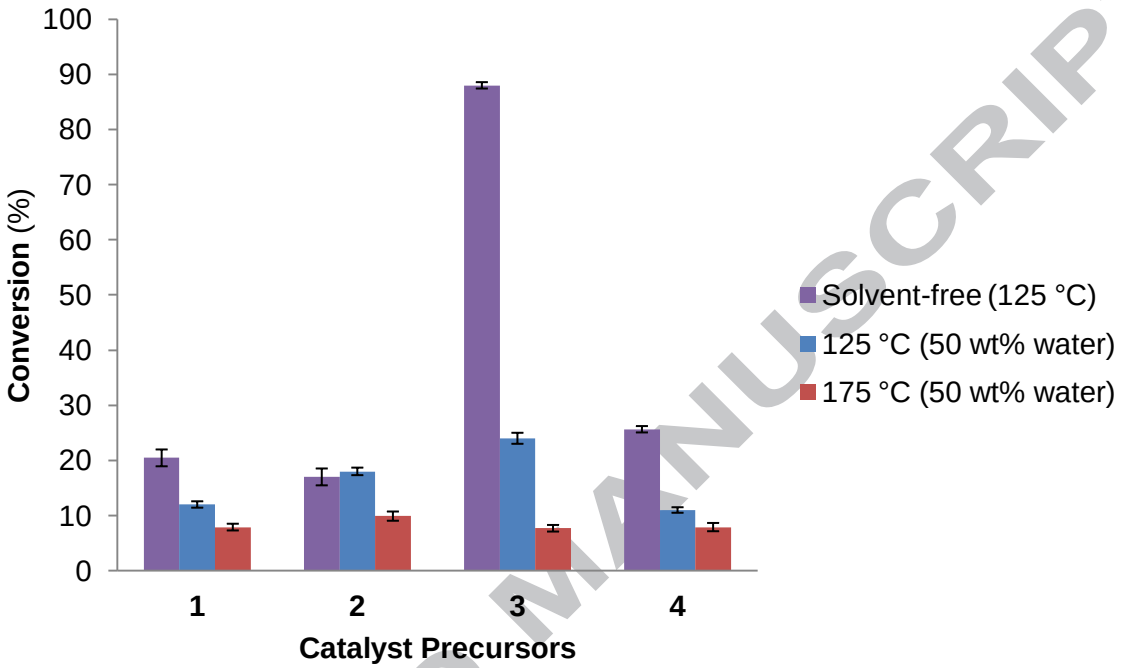

Figure 6: Aqueous hydrogenation of LA using formic acid.

These reductions in conversions may be due to the aquation of the chloride leaving groups on the pre-catalysts which could then be followed by the formation of inactive oxo-bridging species [35,37b]. This aquation of the chloride ligand may further be enhanced at elevated temperatures as is evidence from when the reactions were performed at 175 °C [37b]. Since pre-catalysts **1**, **2** and **3** are soluble in water, it is unlikely that the reduction in conversions might be due to solubility issues.

4. CONCLUSIONS

We have shown that easily prepared (in one step) pyridylimine ligands can be used to synthesize new ruthenium(II) complexes, that are active pre-catalysts for the solvent-free selective hydrogenation of levulinic acid (LA) to γ-valerolactone (GVL) by using formic acid (FA) as the hydrogen source. This is practical since the source of hydrogen, FA, is a by-product in the production of LA. The hydrogen gas was derived from ruthenium-catalysed decomposition of FA and a mechanism for the catalytic reaction has been proposed. The

efficiency of these reactions under solvent-free conditions makes the current hydrogenation reactions green. In addition to this, the catalysts can be recycled up to three times while maintaining 100 % LA conversion and GVL selectivity.

ACKNOWLEDGEMENTS

This work was supported by the University of Johannesburg' Centre for Synthesis and Catalysis, the National Research Foundation of South Africa (NRF) (Grant Numbers: 99269 and 105556) and SASOL LTD. The use of UJ Spectrum's NMR facilities is also acknowledged.

DECLARATIONS OF INTEREST: We declare no conflict of interest in financial support for this work

REFERENCES

[1] J.J. Bozell, Science 329 (2010) 522–523.

[2] Y. Gong, L. Lin, Z. Yan, BioResources 6 (2011) 686–699.

[3] G.M. Joselin Herbert, A. Unni Krishnan, Renew. Sustain. Energy Rev. 59 (2016) 292–308.

[4] (a) K.C. Wu, in:, B. Trewyn (Ed.), Heterog. Catal. Today's Challenges Synth. Charact. Appl., The Royal Society of Chemistry, 2015, pp. 1–27. (b) B.C.E. Makhubela, J. Darkwa, Johnson Matthey Technol. Rev. 62 (2018) 4-31.

[5] X. Zhuang, W. Wang, Q. Yu, W. Qi, Q. Wang, X. Tan, G. Zhou, Z. Yuan, Bioresour. Technol. 199 (2015) 68–75.

[6] M. Mascal, E.B. Nikitin, Green Chem. 12 (2010) 370–373.

[7] S. Dutta, S. Pal, Biomass and Bioenergy 62 (2014) 182–197.

[8] K. Yan, Y. Yang, J. Chai, Y. Lu, Appl. Catal. B Environ. 179 (2015) 292–304.

[9] I.T. Horváth, Green Chem. 10 (2008) 1024–1028.

[10] P. Gallezot, Chem. Soc. Rev. 41 (2012) 1538–1558.

[11] M. Wachala, J. Grams, W. Kwapinski, A.M. Ruppert, Int. J. Hydrogen Energy 41 (2016) 8688–8695.

[12] M.J. Climent, A. Corma, S. Iborra, Green Chem. 16 (2014) 516–547.

[13] L.E. Manzer, Appl. Catal. A Gen. 272 (2004) 249–256.

[14] M.G. Al-shaal, W.R.H. Wright, R. Palkovits, Green Chem. 14 (2012) 1260–1263.

[15] C. Michel, P. Gallezot, ACS Catal. 5 (2015) 4130–4132.

[16] A.M. Hengne, N.S. Biradar, C. V. Rode, Catal. Letters 142 (2012) 779–787.

[17] W. Luo, U. Deka, A.M. Beale, E.R.H. Van Eck, P.C.A. Bruijnincx, B.M. Weckhuysen, J. Catal. 301 (2013) 175–186.

[18] J. Deng, Y. Wang, T. Pan, Q. Xu, Q.X. Guo, Y. Fu, ChemSusChem 6 (2013) 1163–1167.

[19] C. Ortiz-Cervantes, M. Flores-Alamo, J.J. García, ACS Catal. 5 (2015) 1424–1431.

[20] J.H. Barnard, C. Wang, N.G. Berry, J. Xiao, Chem. Sci. 4 (2013) 1234–1244.

[21] W. Li, J.-H. Xie, H. Lin, Q.-L. Zhou, Green Chem. 14 (2012) 2388–2390.

[22] P.D. Gabor Laurenczy, Céline Fellay, J. Am. Chem. Soc. 132 (2010) 8924–8934.

[23] S. Fukuzumi, T. Kobayashi, T. Suenobu, ChemSusChem 1 (2008) 827–834.

[24] A. Boddien, B. Loges, H. Junge, F. Gärtner, J.R. Noyes, M. Beller, Adv. Synth. Catal. 351 (2009) 2517–2520.

[25] L. Deng, J. Li, D. Lai, Y. Fu, Q. Guo, Angew. Chemie - Int. Ed. 48 (2009) 6529–6532.

[26] V. Fábos, L.T. Mika, I.T. Horváth, Organometallics 33 (2014) 181–187.

[27] G. Amenuvor, B.C.E. Makhubela, J. Darkwa, ACS Sustain. Chem. Eng. 4 (2016) 6010–6018.

[28] G.J.P. Britovsek, G.Y.Y. Woo, N. Assavathorn, J. Organomet. Chem. 679 (2003) 110–115.

[29] G. Venkatachalam, R. Ramesh, Inorg. Chem. Commun. 9 (2006) 703–707.

[30] T. Opstal, F. Verpoort, Angew. Chemie - Int. Ed. 42 (2003) 2876–2879.

[31] (a) S. Azizi Talouki, G. Grivani, P. Crochet, V. Cadierno, Inorganica Chim. Acta (2016) 1–7. (b) Caserta Production Plant: Innovation and R&D', GFBIochemicals, Milan, Italy: http://www.gfbiochemicals.com/company/#caserta-plant (Accessed on 12 April 2018)

[32] M.O. Albers, T.V. Ashworth, H.E. Oosthuizen, E. Singleton, J.S. Merola, R.T. Kacmarcik, Inorganic Syntheses, John Wiley and Sons, 1989.

[33] B.P. Buffin, E.B. Fonger, A. Kundu, Inorganica Chim. Acta 355 (2003) 340–346.

[34] B. Roberts, S.J. Harris, M.T.W. Hearn, R.I. Boysen, Chemical Compound Arrays Useful for Detecting Bacterial Peptides, WO2011140599 A1, 2011.

[35] C. Gaiddon, W.H. Ang, M.J. Chow, C. Licona, D.Y.Q. Wong, G. Pastorin, J. Med. Chem. 57 (2014) 6043–6059.

[36] S. Wang, V. Dorcet, T. Roisnel, C. Bruneau, C. Fischmeister, Organometallics 36 (2017) 708–713.

[37] (a) See electronic annex Table S1 (b) É.A. Enyedy, G.M. Bognár, T. Kiss, M. Hanif, C.G. Hartinger, J. Organomet. Chem. 734 (2013) 38–44. (c) See electronic annex l Figure S1. (d) See electronic annex Figure S2. (e) See electronic annex Table S2

[38] T. Zell, B. Butschke, Y. Ben-David, D. Milstein, Chem. - A Eur. J. 19 (2013) 8068–8072.

[39] D. Garce, D. Eva, S. Ordo, Ind. Eng. Chem. Res. 56 (2017) 5221–5230.

Highly Selective and Efficient Solvent-free Transformation of Bio-derived Levulinic acid to γ-Valerolactone by Ruthenium Arene Catalyst Precursors

Novisi K. Oklu[a] and Banothile C. E. Makhubela[a*]

[a]*Department of Chemistry, University of Johannesburg, Auckland Park Kingsway Campus*

P.O. Box 524, South Africa, Johannesburg

[*]E-mail: bmakhubela@uj.ac.za

GRAPHICAL ABSTRACT

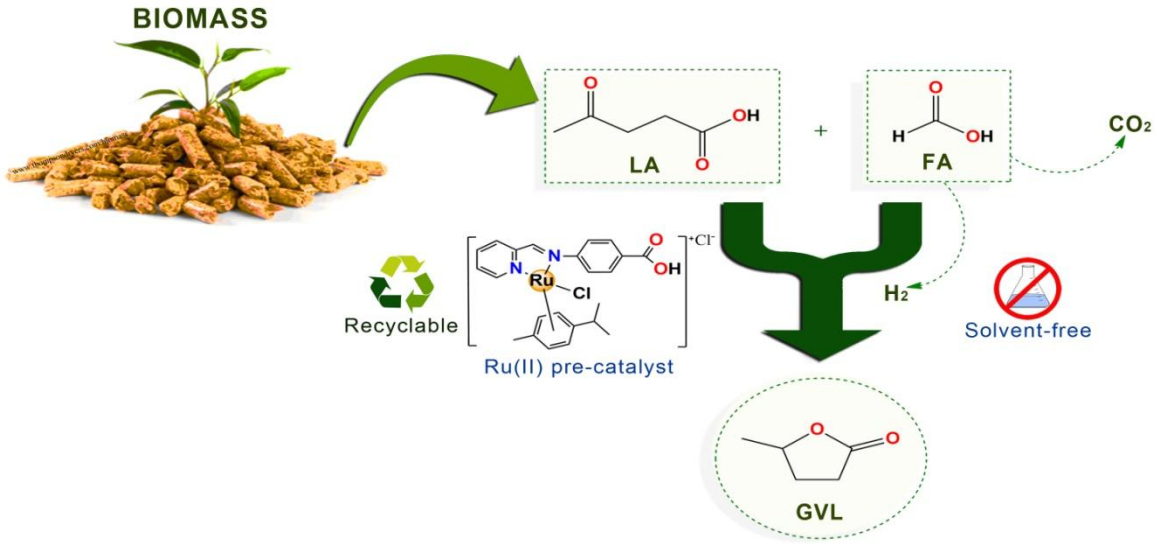

Highly Selective and Efficient Solvent-free Transformation of Bio-derived Levulinic acid to γ-Valerolactone by Ruthenium Arene Catalyst Precursors

Novisi K. Oklu[a] and Banothile C. E. Makhubela[a*]

[a]*Department of Chemistry, University of Johannesburg, Auckland Park Kingsway Campus*

P.O. Box 524, South Africa, Johannesburg

[*]E-mail: bmakhubela@uj.ac.za

HIGHLIGHTS

1. A highly selective method of converting bio-based levulinic acid to γ-valerolactone using formic acid as a hydrogen carrier.
2. Hydrogenation of levulinic acid resulted in 100% conversions and selectivity to γ-valerolactone, and in situ NMR characterization has aided the proposal of a plausible mechanism of the reaction.
3. Ruthenium pre-catalysts catalyze the hydrogenation reactions without the need of a solvent and are also recyclable, thereby making the entire reaction conditions greener.